IEEE Access
Multidisciplinary | Rapid Review | Open Access Journal

Received August 11, 2020, accepted August 19, 2020, date of publication August 28, 2020, date of current version September 10, 2020.

Digital Object Identifier 10.1109/ACCESS.2020.3020095

Kinematics Analysis of 3UPU_UP Coupling Parallel Platform in the Marine Environment

XIONG HU, FURONG LI, AND GANG TANG
Logistics Engineering College, Shanghai Maritime University, Shanghai 201306, China
Corresponding author: Gang Tang (gangtang@shmtu.edu.cn)

This work was supported by the Shanghai Sailing Program under Grant 19YF1419100 and Grant 19YF1418900.

ABSTRACT A study of the kinematic characteristics of a 3UPU_UP coupling parallel platform that has three-degree-of-freedom(3-DOF). In this article, a novel 3UPU_UP parallel platform is presented, which is based on the 5-DOF 3UPU parallel platform by adding a UP followed limb. The DOFs and motion constraints of the platform are analyzed by the screw theory, and the coupling constraint equation of the platform is obtained through coordinate transformation. The inverse kinematics equation of the platform is derived by the closed-loop method, and the forward kinematics equation of the platform is solved by Netwon-Rapson iteration. The trajectory of the platform in space is obtained and the correctness of the coupling constraint equation of the platform in other DOFs is verified. Considering that the motion of a ship on the sea is multi-DOF and complicated, the motion of the cargo on the ship can be compensated by using a coupling characteristic of the platform to improve the safety of marine operations.

INDEX TERMS 3UPU_UP parallel platform, coupled constraint equation, Kinematic analysis, ocean wave model.

I. INTRODUCTION

The parallel platform usually consists of a mobile platform, which is connected to a fixed base by many limbs. The number of limbs is usually equal to the number of degrees of freedom(DOF), and each limb is driven by an actuator. The parallel platform has the advantages of high rigidity, fast response speed, and high control accuracy. Some motion systems composed of it have been applied on some ship simulators and wave compensation platforms [1].

In some engineering applications, not all 6 DOFs need to be used, so many parallel platforms with fewer DOFs were born. Over the past decades, a great number of improvements regarding 3-DOF parallel platforms have been achieved. There are many 3-DOF platforms with different structures, such as 3PUU parallel platforms [2]–[4], 3RPS parallel platforms [5], [6]. The 3UPU parallel platform has also been extensively studied by scholars. Huang and Li [7] summarized a variety of 3UPU parallel platforms, including 5-DOF parallel platform, 3-DOF spherical parallel platform, 3-DOF translation parallel platform, and 4-DOF parallel platform. In principle, the mobility of the moving platform is determined by the layout of linear limbs and the arrangement of universal joints. Assuming that the layout of each UPU limb in the platform is symmetrical, there are four different kinds of mobility situations for different DOFs of the general 3UPU parallel platform. The first case is that the 3-DOF which means to 3 translational DOFs, the second case is the 3-DOF which means to 3 rotational DOFs, the third case is the 4-DOF which means to 3 rotational and 1 translational DOFs, the fourth case is the 5-DOF which means to 3 rotational and 2 translational DOFs. Establish a local coordinate system for each limb and analyze using the screw theory [8]. Each UPU limb is composed of 5 joints, from bottom to top are $R_aR_bP_1R_cR_d$. A universal (U) joint can be seen as two perpendicular revolute (R) joints. The subscript represents the rotational axis or translational axis of each joint. For the case I, if the moving platform needs to meet the 3-DOF translation, it means that the constraint couples generated by the three UPU limbs are linearly independent. The joint of the UPU limb is $R_xR_bP_1R_cR_d$, where the c-axis is parallel to the b-axis and the y-axis. The d-axis is not parallel to the x-axis, forming a 3-DOF translational parallel platform [9], [10]. For case II, if the moving platform needs to meet 3-DOF rotation, it means that the constraint forces generated by the three UPU limbs are linearly independent. The joints of the UPU limb are arranged as $R_xR_yP_1R_cR_d$, where the c-axis is parallel to the y-axis and the d-axis is parallel to

The associate editor coordinating the review of this manuscript and approving it for publication was Yangmin Li.

the x-axis, forming a 3-DOF spherical parallel platform [11]. For case III, if the moving platform needs to meet 3-DOF rotation and 1-DOF translation, it means that the 3 constraint forces formed by the three UPU limbs are co-planar. The joints of the UPU limb are $R_xR_zP_1R_cR_d$, where the c-axis is parallel to the z-axis and the d-axis parallel to the x-axis, forming a 4-DOF parallel platform [7]. For case IV, if the moving platform needs to meet 3-DOF rotation and 2-DOF translation, it means that the 3 constraint couples formed by the three UPU limbs are co-linear. The joints of the UPU limb are arranged as $R_xR_yP_1R_cR_d$, where the c-axis is parallel to the y-axis and the d-axis is parallel to the x-axis, forming a 5-DOF parallel platform with a common constraint. Yang and Li [12] used this type of UPU limbs to build a 5-DOF parallel platform. To achieve 5 DOFs motion, it is necessary to ensure that the axis of the moving platform in the initial pose should be perpendicular to the base and the moving platform at the same time. Case IV is a special arrangement of case II. Sarabandi *et al.* [13] proposed a 3UPU platform that can reconfigure its motion. By changing the assembly condition of the UPU limb in the platform, the platform can be turned into a translational platform or a spherical platform.

The modified Grübler-Kutzbach criterion [14] can be used for the analysis of the freedom of the platform. The kinematic modeling of the platform can use its closed-loop characteristics based on its structure [15]. The inverse kinematics of the parallel platform is simple, while the solution of the forward kinematics is more complicated. The solution of positive kinematics can be solved by Netwon-Rapson iteration [16]. Bhutani and Dwarakanath [17] studied the kinematics of the 3UPU parallel platform with translation only, analyzed singularity, and get the singularity-free workspace. Lu *et al.* [18] analyzed the kinematics of two 3UPU parallel platforms with different structures, and obtained the displacement, velocity, acceleration, and workspace of the two structures. Shafiee-Ashtiani *et al.* [19] studied the forward and inverse solutions of the kinematics of the 3UPU platform and proposed a fast and effective new method.

The kinematics research of the 3UPU parallel platform mainly focuses on the analysis of the kinematics forward solution, inverse solution, working space, and singular points and singular configuration, but due to the complexity of the parallel platform structure, it often produces a certain coupling effect [20]. This coupling effect often limits the control performance of some control algorithms for parallel platforms. Carretero *et al.* [21] optimizes the structure size of the parallel platform, and its optimization goal is that the motion of the platform has certain coupling characteristics, that is, the additional motions of other DOFs will be generated. Luo *et al.* [22] propose a coupling type parallel platform, which utilizes the coupling characteristics of a marine vessel to apply the platform to a landing of a Marine helicopter. To further study the motion of cargo and ship in the marine environment, the Pierson-Moscowitz (P-M) spectrum [23], [24] can be used to construct the ocean wave model.

This article studies the kinematics analysis of 3UPU_UP coupled parallel platforms in the marine environment. The platform is constructed by adding a UP followed limb base on the 5-DOF 3UPU parallel platform. In Section II, through the screw theory and modified Grübler-Kutzbach criterion, the kinematic characteristics and DOFs the platform are analyzed. In Section III, the coupling constraint equation of the platform is solved by a coordinate transformation. The inverse kinematics is solved using the closed-vector method and the forward kinematics is solved using Netwon-Rapson iteration. In Section IV, the structural parameters and input signals of the platform are given for simulation analysis. Considering the multi-DOF coupling characteristics of ships at sea, the ocean wave data generated by the P-M spectrum is input to the platform for analysis. The trajectory and coupling displacement of the platform under a given signal is obtained. Conclusions are drawn in Section V.

II. PLATFORM DESCRIPTION AND MECHANISM ANALYSIS

A. 3UPU PARALLEL PLATFORM WITH 5-DOF

The 5-DOF 3UPU parallel platform includes a base, a moving platform, and three UPU limbs. Among them, U represents the universal joint, which can be regarded as two intersecting rotating joints and P is a prismatic joint as an actuator. Each UPU limb has five joints, which are $R_uR_vP_1R_cR_d$. In this platform, the three UPU limbs are arranged in the same direction and each limb is separated by 120°. The c-axis is parallel to the v-axis and the d-axis is parallel to the u-axis. The translation axis of the prismatic joint is perpendicular to the base and the moving platform which can form a 3UPU parallel platform. As shown in Fig.1.

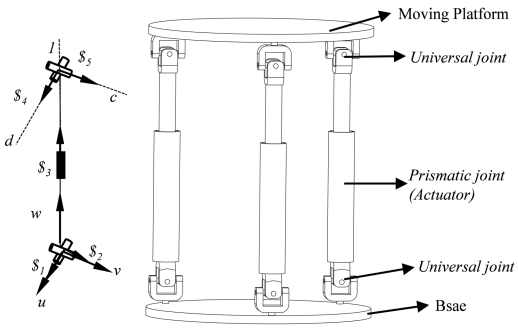

FIGURE 1. 3UPU parallel platform with 5-DOF.

In screw theory, the general form of a screw is given by $\$ = (s; r \times s)$, where s is a unit vector along the screw axis, r is the position vector of any point on the screw axis. The unit screw associated with a revolute joint is given by $\$ = (s; r \times s) = (l\ m\ n; a\ b\ c)$, where l, m, n denotes the three direction cosines of the revolute axis. The unit screw associated with a prismatic joint is given by $\$ = (s; r \times s) = (0\ 0\ 0; l\ m\ n)$. The screw system of single UPU limb in the local coordinate

system at the original configuration is:

$$\begin{cases} \$_1 = (1\ 0\ 0; 0\ 0\ 0) \\ \$_2 = (0\ 1\ 0; 0\ 0\ 0) \\ \$_3 = (0\ 0\ 0; 0\ 0\ 1) \\ \$_4 = (1\ 0\ 0; 0\ -l\ 0) \\ \$_5 = (0\ 1\ 0; l\ 0\ 0) \end{cases} \tag{1}$$

where l represents the distance between the center of two U joints. The screw system has five linearly independent screws. Assuming there are reciprocal screws $\$_i^r = (L_i^r\ M_i^r\ N_i^r; P_i^r\ Q_i^r\ R_i^r)$, according to the following formula:

$$\$ \circ \$_i^r = 0 \tag{2}$$

the reciprocal screw of this UPU limb can be solved as $\$_{11}^r = (0\ 0\ 0; 0\ 0\ 1)$. It can be seen from the reciprocal screw that there is a constraint couple on the z-direction. Due to the presence of the constraint couple, the rotation of the platform in the z-axis is restricted. Because of the same structure, each limb will produce a constraint couple. When three constraint couples are co-linear, there will be a common constraint, which can only limit the rotation of the moving platform around the z-axis. The modified Grübler-Kutzbach criterion for calculating the DOFs is as follows:

$$M = d(n - g - 1) + \sum_{i=1}^{h} f_i + \nu \tag{3}$$

where M represents the DOFs of a mechanism, $d = 6 - \lambda$ represents the DOFs of the space, λ represents the common constraint, n represents the total number of components, g represents the number of motion joints, f_i represents the DOFs of the i-th motion joint. ν represents the number of redundant constraints after subtracting the common constraints.

According to Fig.1, the total number of components of the platform is 8; the three UPU limbs are divided into upper and lower components, a moving platform, a base. The number of motion joints is 9, 6 U joints have a total of 12 DOFs, 3 P joints have 3 DOFs. There is still a common constraint. Except for the common constraints, there are no other constraints and $\nu = 0$. By substituting the relevant parameters, the calculation results are as follows:

$$M = (6 - 1) * (8 - 9 - 1) + 3 * (2 + 1 + 2) + 0 = 5 \tag{4}$$

B. 3UPU_UP COUPLED PARALLEL PLATFORM WITH 3-DOF

According to (4), the parallel platform has three actuators and 5 DOFs, so it will produce uncertain motion. Therefore, based on Fig.1, a followed UP limb is added to reduce the DOFs of the 3UPU platform to construct a coupled 3-DOF parallel platform. As shown in Fig.2, a UP limb is arranged in the center of the base, where the U joint is connected to the base and the P joint is connected to the moving platform. The first rotation axis of the U joint is parallel to the first and fifth rotation axis in each UPU limb. The second rotation axis of the U joint is parallel to the second and third rotation axis in each UPU limb. The translation axis of the P joint is parallel to the other three translation axis in the initial position.

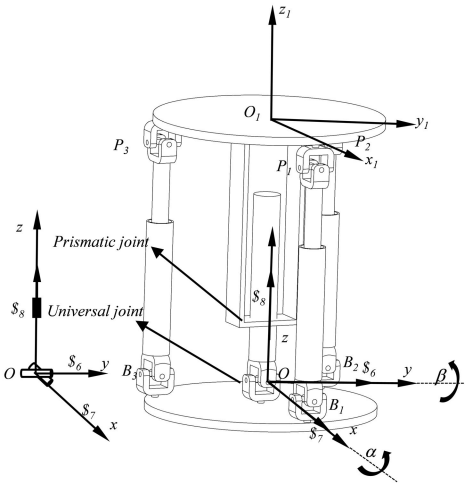

FIGURE 2. 3UPU_UP coupled parallel platform with 3-DOF.

For a better analysis of the platform, the coordinate systems $O - xyz$ is located on the base, and the coordinate systems $O_1 - x_1y_1z_1$ is located on the moving platform. P_i represents the center point of the upper U joint of the i-th UPU limb, B_i represents the center point of the lower U joint of the i-th UPU limb. The constructed 3-DOF coupling platform with 2 rotation and 1 translation is shown in Fig.2. The screw system of the followed UP limb in the local coordinate system at the original configuration is:

$$\begin{cases} \$_6 = (0\ 1\ 0; 0\ 0\ 0\ ) \\ \$_7 = (1\ 0\ 0; 0\ 0\ 0) \\ \$_8 = (0\ 0\ 0; 0\ 0\ 1) \end{cases} \tag{5}$$

According to (2), we can get the reciprocal screws of the screw system:

$$\begin{cases} \$_{21}^r = (0\ 0\ 0; 0\ 0\ 1) \\ \$_{22}^r = (1\ 0\ 0; 0\ 0\ 0) \\ \$_{23}^r = (0\ 1\ 0; 0\ 0\ 0) \end{cases} \tag{6}$$

It can be seen from the reciprocal screws of the screw system that there are two constraint forces and one constraint couple. These two constraint forces limit the translation of the moving platform in the x-axis and y-axis, respectively, and the constraint couple restricts the rotation of the moving platform around the z-axis. Combined with the content of the above analysis, since the four limbs all have upward restraint couples on the moving platform, the 3UPU-UP platform also has a common constraint. At the same time, the platform has a total of 9 components and 11 joints. Except for the common constraint, there are two linearly independent constraints, so there is also no redundant constraint and $\nu = 0$. According to the (3), the DOFs of the platform is as follows:

$$M = (6-1) * (9-11-1) + 3 * (2+1+2) + 2 + 1 + 0 = 3 \tag{7}$$

This new platform with the 3UPU and UP limbs provides 3 DOFs, namely, heave z, vertical translation of moving platform along the z-axis, roll α, rotation of moving platform around the x-axis and pitch β, rotation of moving platform around the y-axis. The platform has two continuous rotation axis and the position of the rotation axis is related to the constraint forces, so it can be known that the rotation axis of the platform is the same as the two rotation axis of the U joint in the followed UP limb.

III. KINEMATICS MODELING OF THE PLATFORM

A. COUPLED CONSTRAINT EQUATION

The position and direction of the moving platform relative to the reference coordinate system in space need to be described by six variables, that is $A_1 = (x, y, z, \alpha, \beta, \gamma)$, the position and direction of the point relative to the reference coordinate system. Due to 3UPU_UP is a 3-DOF platform, so the input of the platform has only three parameters which are (z, α, β). Due to the coupling characteristics of the parallel platform, the constraint equation of the platform in other directions can be obtained.

Suppose A_1 is an arbitrary point on the moving platform, where l represents the coordinate of the point on the z-axis. Assuming that the moving platform can move in 3 DOFs on the base coordinate system. Point A_1 will get a new point A_2 after rotating and translating, as shown in Fig.3, Fig.4, and Fig.5.

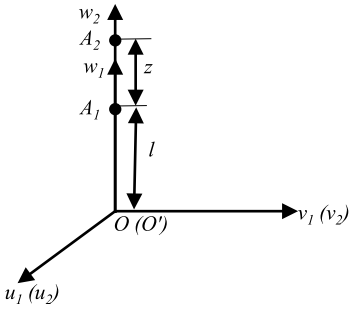

FIGURE 3. The position transformation relationship of translation along the z-axis.

It can be seen from Fig.3 that when the moving platform moves z along the z-axis, there will be no coupling motion. The new position is:

$$A_2 = (x_1.y_1, l + z) \tag{8}$$

It can be seen from Fig.4 that when the moving platform rotates around the x-axis by α, a certain coupling motion will occur on the y-axis and the z-axis. The new position is:

$$A_2 = (x_1.y_1 cos\alpha - lsin\alpha, y_1 sin\alpha + lcos\alpha) \tag{9}$$

It can be seen from Fig.5 that when the moving platform rotates around the y-axis by β, a certain coupling motion will occur on the x-axis and the z-axis. The new position is:

$$A_2 = (x_1 cos\beta, y_1, x_1 sin\beta + lcos\beta) \tag{10}$$

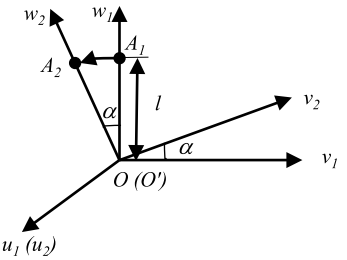

FIGURE 4. The position transformation relationship of rotation around the x-axis.

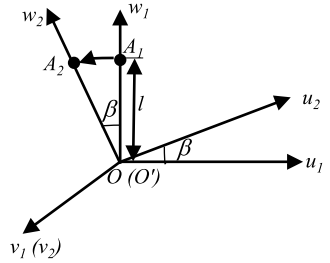

FIGURE 5. The position transformation relationship of rotation around the y-axis.

When a point on coordinate system $O_1 - x_1y_1z_1$ performs a 3 DOFs motion in the coordinate system $O - xyz$, a transformation matrix converted from dynamic coordinate system $O_1 - x_1y_1z_1$ to coordinate system $O - xyz$ is as follows:

$$^{O}T_{O_1} = \begin{bmatrix} \cos\beta & 0 & \sin\beta & X_p \\ \sin\alpha\sin\beta & \cos\alpha & -\sin\alpha\cos\beta & Y_p \\ -\cos\alpha\sin\beta & \sin\alpha & \cos\alpha\cos\beta & Z_p \\ 0 & 0 & 0 & 1 \end{bmatrix} \tag{11}$$

Since (11) is a 4×4 matrix and the coordinate is a 3×1 matrix, it is necessary to generalize the coordinates of A_1 before an operation. Bringing any point in the moving platform into it, the coupling constraint equation of the platform in other DOFs can be obtained as follows:

$$\begin{cases} X_p = x_1\cos\beta + (l+z)\sin\beta \\ Y_p = x_1 sin\alpha sin\beta + y_1 cos\alpha - (l+z) sin\alpha cos\beta \\ Z_p = -x_1 cos\alpha sin\beta + y_1 cos\beta sin\alpha + (l+z) cos\alpha cos\beta \end{cases} \tag{12}$$

It can be seen from the above results that coupling constraints are generated in the three translation directions, and corresponding additional motions are generated. To simplify the motion model, we select the center of mass of the moving platform for analysis, so the constraint equation of the platform can be simplified to the following formula:

$$\begin{cases} X_p = (l+z)\sin\beta \\ Y_p = -(l+z) sin\alpha cos\beta \\ Z_p = (l+z) cos\alpha cos\beta \end{cases} \tag{13}$$

Therefore, the actual position and direction of the point on the platform is expressed as:

$$P_2 = (X_p, Y_p, Z_p, \alpha_p, \beta_p) \tag{14}$$

Equation (13) shows that the coupling characteristics of the platform will not affect the rotation angle of the moving platform, but will affect the translational motion. Use output position minus input position to obtain coupled displacement:

$$\begin{aligned} D_c &= (X_c, Y_c, Z_c) \\ &= (X_p - 0, Y_p - 0, Z_p - (l + z)) \end{aligned} \tag{15}$$

X_c, Y_c, Z_c represents the coupling displacement of the moving platform on the x-axis, y-axis, and z-axis respectively.

B. INVERSE KINEMATICS

A closed-loop method is used to extract the characteristics of a UPU limb in a parallel platform. As shown in Fig.6. According to Fig.6, the closed-loop equation of each limb can be obtained as:

$$\vec{l_i} = \vec{r_p} + \vec{p_i} - \vec{b_i} \tag{16}$$

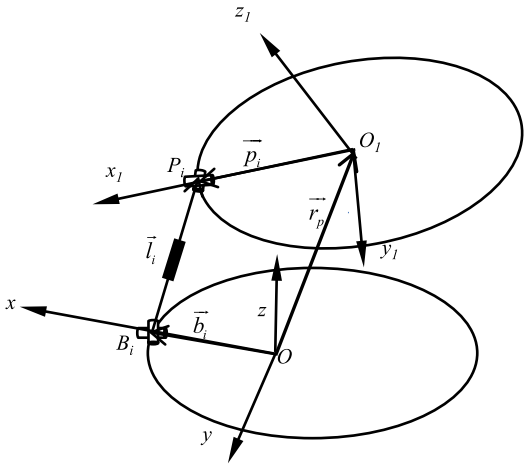

FIGURE 6. Closed-loop of a UPU limb.

where $\vec{l_i}$ is the vector between the center points of the two U joints in each UPU limb. $\vec{r_p}$ is the vector from the center O in the inertial coordinate system $O - xyz$ to the center O_1 of the moving platform. $\vec{b_i}$ is the vector from the center O to B_i in the inertial coordinate system which is a fixed vector, $\vec{p_i}$ is the same as the vector between the center O_1 and p_i in the dynamic coordinate system $O_1 - x_1y_1z_1$. z represents the translation along the z-axis, and α, β represents the rotation around the x-axis and the y-axis. According to (11), the coordinates of the points on the $O_1 - x_1y_1z_1$ can be transformed to the $O - xyz$.

$$\left(\frac{^{O}P}{1}\right) = {}^{O}T_{O_1}\left(\frac{^{O_1}P}{1}\right) \tag{17}$$

Therefore, the length of each limb can be derived according to the given parameter and (16):

$$l_i = \sqrt{(^{O}P_i - ^{O}b_i)^{\mathrm{T}}(^{O}P_i - ^{O}b_i)} \tag{18}$$

By using the obtained length of each limb minus the original length, the changing relationship of each limb during motion can be obtained, where l is the length of each limb at the initial pose of the platform.

$$\begin{cases} \Delta l_1 = l_1 - l \\ \Delta l_2 = l_2 - l \\ \Delta l_3 = l_3 - l \end{cases} \tag{19}$$

C. FORWARD KINEMATICS

By deforming the (18), the system of nonlinear equations for solving forward kinematics is obtained:

$$f_i(z, \alpha, \beta) = \left[(^{O}P_i - ^{O}b_i)^{\mathrm{T}}(^{O}P_i - ^{O}b_i)\right] - l_i^2 \tag{20}$$

Let (20) be solved as:

$$x^* = [z_1, \alpha_1, \beta_1]^{\mathrm{T}} \tag{21}$$

Select the initial value $x_k = [z_k, \alpha_k, \beta_k]^{\mathrm{T}}$ near the solution to be solved, then:

$$x^* = x_k - \delta \tag{22}$$

where δ is the error vector, $\delta = [\delta_1, \delta_2, \delta_3]^{\mathrm{T}}$, the following equations can be obtained:

$$\begin{cases} f_1(z_k - \delta_1, \alpha_k - \delta_2, \beta_k - \delta_3) = 0 \\ f_2(z_k - \delta_1, \alpha_k - \delta_2, \beta_k - \delta_3) = 0 \\ f_3(z_k - \delta_1, \alpha_k - \delta_2, \beta_k - \delta_3) = 0 \end{cases} \tag{23}$$

Expanding the three equations of (23) according to the Taylor series, and ignoring all partial derivatives above the second order, we have the following matrix form:

$$\begin{bmatrix} f_1 \\ f_2 \\ f_3 \end{bmatrix} = \begin{bmatrix} \frac{\partial f_1}{\partial z} & \frac{\partial f_1}{\partial \alpha} & \frac{\partial f_1}{\partial \beta} \\ \frac{\partial f_2}{\partial z} & \frac{\partial f_2}{\partial \alpha} & \frac{\partial f_2}{\partial \beta} \\ \frac{\partial f_3}{\partial z} & \frac{\partial f_3}{\partial \alpha} & \frac{\partial f_3}{\partial \beta} \end{bmatrix} \times \begin{bmatrix} \delta_1 \\ \delta_2 \\ \delta_3 \end{bmatrix} \tag{24}$$

Bring the selected initial value $x_k = [z_k, \alpha_k, \beta_k]^{\mathrm{T}}$ into the Jacobian matrix on the left and right of the (24), and use the method of solving the linear equation system to obtain the value of the error vector δ, and then solve according to (22) to get x_{k+1}. This solution is better than x_k. Then use x_{k+1} as the initial value to repeat the solution and use (24) to correct it, and iterate repeatedly until $f(x_{k+r} \leq \varepsilon)$. ε is the predetermined deviation value, and the corresponding $x_{k+r} = [z_{k+r}, \alpha_{k+r}, \beta_{k+r}]^{\mathrm{T}}$ is the result of the solved kinematics solution for the given length of the limb. According to the coupling constraint equation (13), the position and direction of the moving platform can be obtained as:

$$\begin{aligned} x_{k+r} = [&(l + z_{k+r})sin\beta_{k+r}, -(l + z_{k+r})sin\alpha_{k+r}cos\beta_{k+r}, \\ &(l + z_{k+r})cos\alpha_{k+r}cos\beta_{k+r}, \alpha_{k+r}, \beta_{k+r}]^{\mathrm{T}} \end{aligned} \tag{25}$$

IV. KINEMATICS SIMULATION AND RESULT ANALYSIS

Establish the kinematics model of the platform according to Fig.2, the basic parameters are as follows:

$$\begin{cases} {}^{O}P = [0, 0, l]^{\mathrm{T}} \\ {}^{O}B_1 = {}^{O_1}P_1 = [\frac{\sqrt{3}}{3}d, 0, 0]^{\mathrm{T}} \\ {}^{O}B_2 = {}^{O_1}P_2 = [-\frac{\sqrt{3}}{6}d, \frac{d}{2}, 0]^{\mathrm{T}} \\ {}^{O}B_3 = {}^{O_1}P_3 = [-\frac{\sqrt{3}}{6}d, -\frac{d}{2}, 0]^{\mathrm{T}} \end{cases} \tag{26}$$

where $l = 1040$mm is the length of each UPU limb in the initial pose, $d = 990$mm is the straight-line distance of every two UPU limb on the base. P_1 represents the center point of the upper U joint of the first UPU limb, B_1 represents the center point of the lower U joint of the first UPU limb. By analogy, other points represent the position of other UPU limbs in the platform. The added UP followed limb is installed at the midpoint of the triangle surrounded by three UPU limbs.

$$\begin{cases} \alpha_1 = R_1 sin(t) \\ \beta_1 = R_2 sin(t) \\ z_1 = D\sin(t) \end{cases} \tag{27}$$

Using (27) as the motion law of the moving platform in each direction. Where $R_1 = R_2 = 5°$, $D = 30$mm. Then taking (27) and (18) into (19), the graphs of the Δl_1, Δl_2, and Δl_3 in three cases can be obtained, as shown in Fig.7.

A. INVERSE KINEMATICS OF SINGLE-DOF UNDER SINE SIGNALS

Fig.7 shows the kinematic characteristics of the three limbs under a single-DOF motion in heave, roll, and pitch are as follows:

(1) Heave motion: Three limbs synchronized motion.

(2) Roll motion: Limb 1 is stationary, limb 2, limb 3 motion in opposite directions with equal amplitude and frequency.

(3) Pitch motion: Limb 2 and limb 3 are synchronized, limb 1 performs equal-frequency, unequal amplitude reverse motion. According to the characteristics of the triangular platform. the amplitude of limb 1 is twice that of limb 2 and limb 3.

B. INVERSE KINEMATICS OF MULTI-DOF UNDER SINE SIGNALS

Since the parallel platform has 3 independent DOFs, there are four kinds of coupling conditions for multi-DOF coupling. Three cases of 2 DOFs coupling and one case of 3 DOFs coupling are as follows:

(1) Coupling of roll direction α and pitch direction β;

(2) Coupling of roll direction α and heave direction z;

(3) Coupling of pitch direction β and heave direction z;

(4) 3-DOF coupling in roll direction α, pitch direction β, and heave direction z;

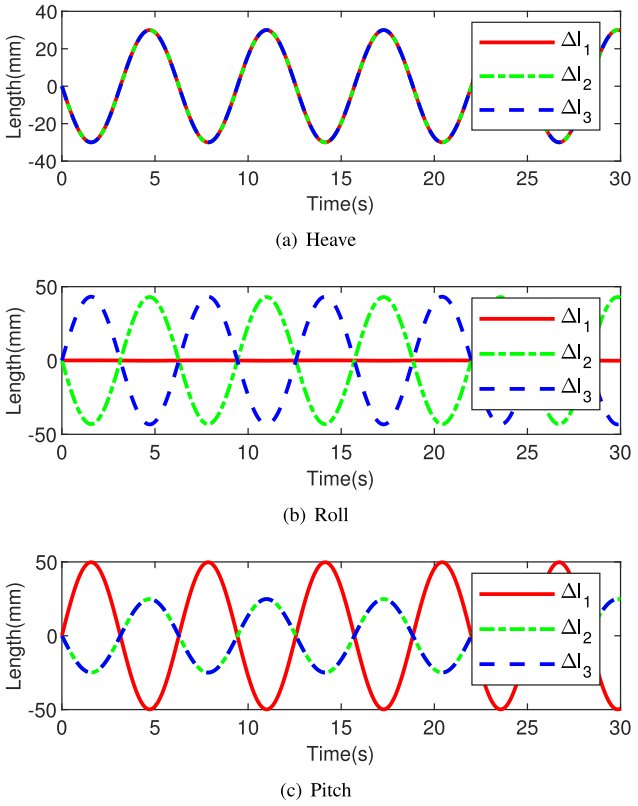

FIGURE 7. Changes in the length of three limbs under a single-DOF.

The above simulation values of α, β, and z are given in (27). According to the given motion law, the inverse solution of the position and attitude of the multi-DOF coupled motion can obtain the graphs of the Δl_1, Δl_2, and Δl_3 in four cases, as shown in Fig.8.

Comparing Fig.7 and Fig.8, it can be found that the relationship between the inverse kinematics solutions of single-DOF and multi-DOF is linear. That is, the inverse kinematics curve under the coupling of roll and pitch can be obtained by adding the inverse kinematics curves of roll and pitch in a single-DOF. The situation is similar for other types of multi-DOF coupled motions

C. CONSTRUCTION OF THE OCEAN WAVE MODEL

Because the ship's motion in the ocean also has a multi-DOF coupling motion, so using the coupling characteristics of the 3UPU_UP platform, the ship's motion can be compensated with fewer DOF. The 3UPU_UP parallel platform is used for ocean wave motion simulation and the kinematics of the platform under multi-DOF coupling is further studied. This article uses the P-M spectrum, and its basic expression is:

$$S(\omega) = \mu\frac{g^2}{\omega^5}\exp\left\{-\rho[\frac{g^2}{U\omega}]^4\right\} \tag{28}$$

where $\mu = 0.0081$, $\rho = 0.74$, g is the acceleration of gravity, g=9.8m/s^2 and U is the wind speed at 19.5m from the sea.

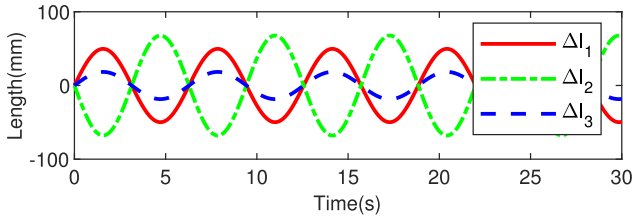

(a) Coupling motions of roll and pitch

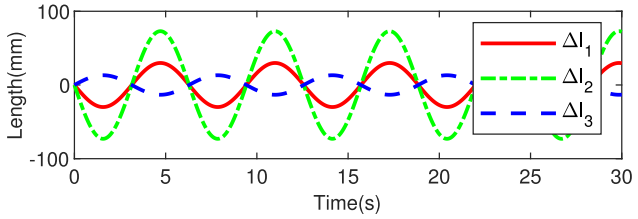

(b) Coupling motions of roll and heave

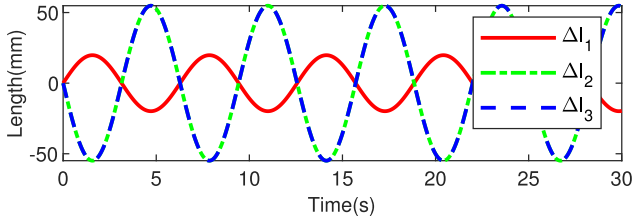

(c) Coupling motions of pitch and heave

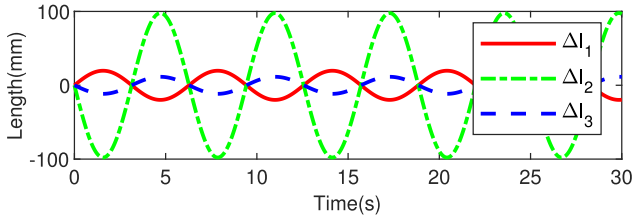

(d) Coupling motions of roll, pitch, and heave

FIGURE 8. Changes in the length of three limbs under a multi-DOF.

According to the energy relationship, the frequency-time domain conversion of the wave simulation curve can be achieved. For a single component wave, the relationship between the amplitude A_i, the slope of wave surface a_i and the wave energy $S(\omega)$ is as follows:

$$A_i = \sqrt{2\Delta\omega S(\omega_i)} \tag{29}$$

$$a_i = \frac{\omega_i^2}{g}\sqrt{2\Delta\omega S(\omega_i)} \tag{30}$$

In this article, the waves in the level-four sea state are modeled and the following parameters are determined by querying the data: the wind speed of the middle-level sea state is 19.5m away from the sea surface and the wind speed is 12m/s. The range of ω is 0.5 to 2.4 rad/s, $\Delta\omega = 0.01$. Bringing in (29) and (30), we can calculate the undulating height function $A(t)$ and slope of wave surface function $a(t)$ under the four-level sea state with wind speed of 12m/s. The result obtained by taking 500 seconds of data is shown in Fig.9:

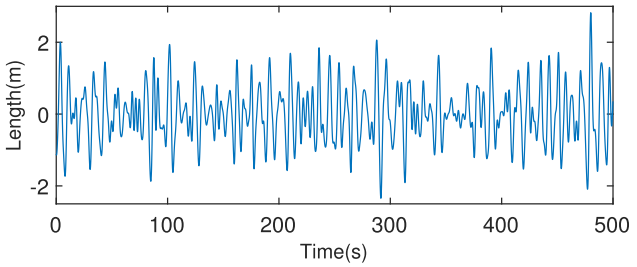

(a) Wave height in level-four sea state

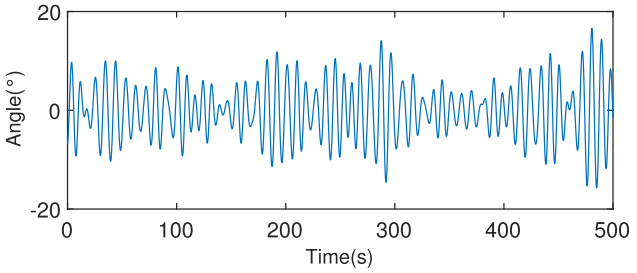

(b) Slope of wave surface in level-four sea state

FIGURE 9. Ocean wave model in level-four sea state.

D. FORWARD KINEMATICS

1) FORWARD KINEMATICS UNDER SINE SIGNALS

The length of each limb under a given motion law is obtained by the (16), and then the actual position and direction are obtained through the Netwon-Raphson iterative. Equation (20) is a complex set of nonlinear equations, so there are certain errors in the iterative algorithm. When solving, set the error accuracy to 10^{-4}. Substituting the motion law in (27) into the algorithm for solving, it can get five parameters in the equation, including: X_p, Y_p, Z_p, α_p, β_p. By expressing these five parameters in space, the trajectory of the platform in space can be obtained, as shown in Fig.10. The conditions corresponding to each trajectory are shown in Table 1.

TABLE 1. The corresponding trajectory of the moving platform under different input sine signals.

Trajectory	Input		
P_1	$\alpha = \alpha_1$	$\beta = \beta_1$	$z = 0$
P_2	$\alpha = 0$	$\beta = \beta_1$	$z = z_1$
P_3	$\alpha = \alpha_1$	$\beta = 0$	$z = z_1$
P_4	$\alpha = \alpha_1$	$\beta = \beta_1$	$z = z_1$

It can be found from Fig.10 that the trajectories of the four coupling modes and the corresponding coupling motion under the given motion law. Through Fig.b, it can be seen that trajectories P_1 is similar to trajectories P_4, all of which generate corresponding motion in the x-axis, y-axis, and z-axis. The difference is that the coordinates of the endpoints of trajectory P_4 are larger than the trajectory P_1. From (13), it can be seen that this result is due to the z-direction motion of trajectory P_4. Through Fig.c, trajectories P_2 on z-axis is slightly larger than the trajectory P_4. The comparison (13) shows that it is because the constraint equation of trajectory P_4 on z-axis multiplies $cos\beta$. The position parameters of

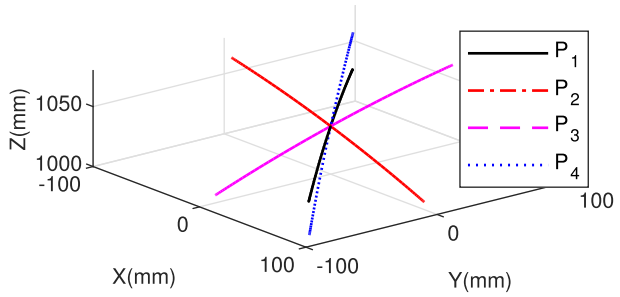

(a) The kinematic trajectory in space

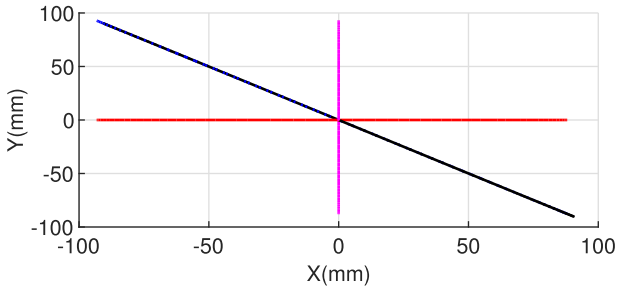

(b) The kinematic trajectory in the XY plane

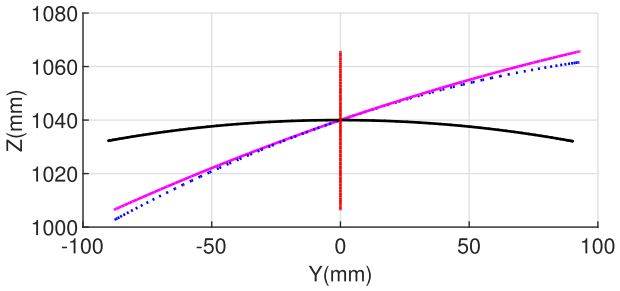

(c) The kinematic trajectory in the YZ plane

FIGURE 10. The kinematic trajectory of four kinds of coupling modes of the moving platform under sine signals.

TABLE 2. The actual position and direction of the moving platform (partial).

(α,β,z)(deg,deg,mm)	$(X_p,Y_p,Z_p,\alpha_p,\beta_p)$(mm,mm,mm,deg,deg)
(5, 5, 0)	(90.6413, -90.3200, 1032.2488, 5.0000, 5.0000)
(5, 0, 30)	(0.0041, -93.2276, 1065.7433, 4.9993, 0.0006)
(0, 5, 30)	(93.2416, -0.0003, 1065.8653, -0.0002, 4.9995)
(5, 5, 30)	(93.2161, 92.8308, 1061.6206, 4.9974, 5.0180)

TABLE 3. The ideal position and direction of the moving platform (partial).

(α,β,z)(deg,deg,mm)	$(X_p,Y_p,Z_p,\alpha_p,\beta_p)$(mm,mm,mm,deg,deg)
(5, 5, 0)	(90.6420, -90.2971, 1032.0962, 5.0000, 5.0000)
(5, 0, 30)	(0.0000, -93.2566, 1065.9342, 5.0000, 0.0000)
(0, 5, 30)	(93.2566, 0.0000, 1065.9342, 0.0000, 5.0000)
(5, 5, 30)	(93.2566, -92.9018, 1061.8684, 5.0000, 5.0000)

some points in the four trajectories can be shown in Table 2. Table 3 is obtained by solving the coupling constraint equation.

By comparing Table 2 and Table 3, it can be found that the ideal position and direction calculated by the constraint equation are very close to the results obtained by the Netwon-Rapson iteration method. The maximum error of the translational motion is about 10^{-2}mm, and the maximum error of the rotational angle is about 10^{-4} degree. According to the (15), the coupling displacement of the parallel platform in the z-axis can also be obtained. The coupling displacement is related to the height of the moving platform and the angle of rotation. The maximum coupling displacement of the P_1 trajectory is 7.9594 mm. The maximum coupling displacement of the P_2 trajectory is 4.0471mm. The maximum coupling displacement of the P_3 trajectory is 4.1346 mm. The maximum coupling displacement of the P_4 trajectory is 8.1706mm.

2) FORWARD KINEMATICS UNDER OCEAN WAVE SIGNALS

Input the ocean wave signals constructed in (29) and (30) to the 3UPU_UP parallel platform. The conditions corresponding to each trajectory are shown in Table 4.

TABLE 4. The corresponding trajectory of the moving platform under different input ocean wave signals.

Trajectory	Input		
P_5	$\alpha = a(t)$	$\beta = a(t)$	$z = 0$
P_6	$\alpha = 0$	$\beta = a(t)$	$z = 0.05A(t)$
P_7	$\alpha = a(t)$	$\beta = 0$	$z = 0.05A(t)$
P_8	$\alpha = a(t)$	$\beta = a(t)$	$z = 0.05A(t)$

Through inverse kinematics solution and Netwon-Raphson iterative solution it can get five parameters in the equation, including: X_p, Y_p, Z_p, α_p, β_p. By expressing these five parameters in space, the trajectory of the platform in space can be obtained, as shown in Fig.11. Since the wave height of the ocean wave signals is in units of m, and the actual motion

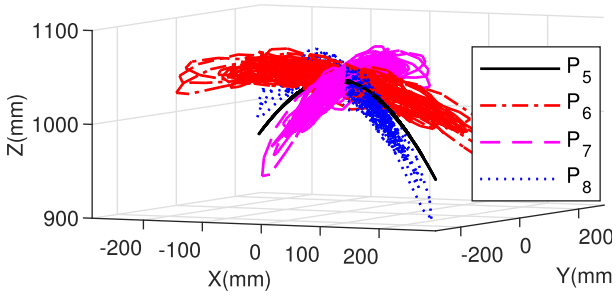

(a) The kinematic trajectory in space

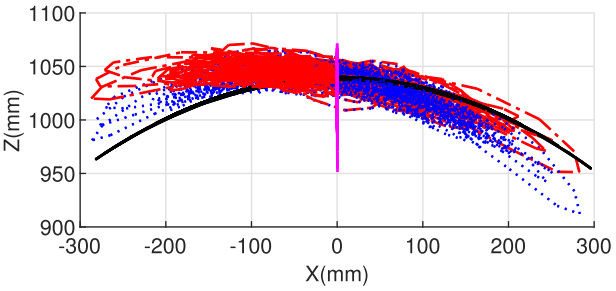

(b) The kinematic trajectory in the XZ plane

FIGURE 11. The kinematic trajectory of four kinds of coupling modes of the moving platform under ocean wave signals.

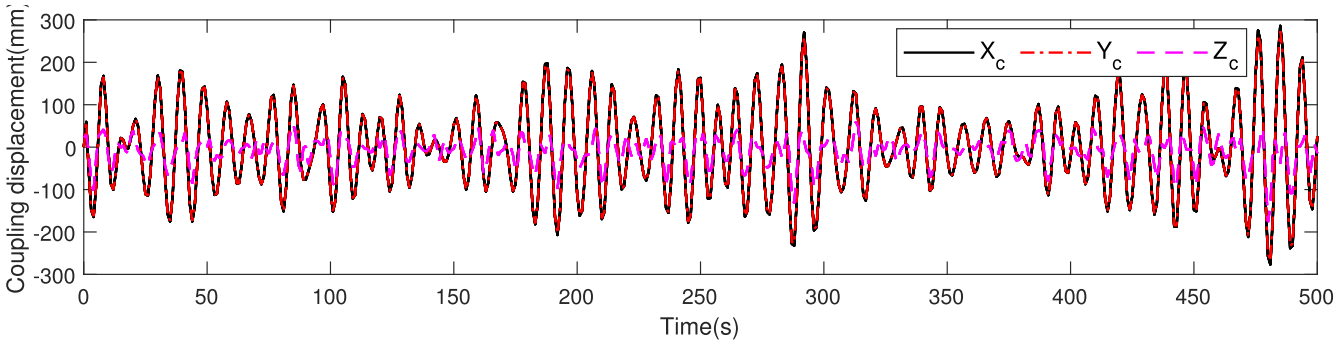

FIGURE 12. The coupling displacement curve of 3UPU_UP platform in three directions under the ocean wave signals.

of the ship in the heave direction is not so large. Therefore replace the heave displacement z with 0.05 times the wave height signals of the level-four sea state and the slope of wave surface is as the roll angle α and the pitch angle β.

Compared with Fig.10 and Fig.11, it can be found that there is a certain similarity in the kinematic trajectory of the multi-DOF coupling under two different signals. The difference is that the ocean wave signals are called a superposition of a series of sine signals with different amplitudes and frequencies, while the signals in Fig.10 are simple sine signal with a single frequency and amplitude. Therefore, the trajectory of the moving platform under the wave signals is the trajectory of multiple line segments. Because the amplitude of the ocean wave signal is larger than the sine signal, the coupling displacement produced by the wave signal is also larger than the coupling displacement produced by the sine signal.

In order to see the coupling displacement under the ocean wave signals more intuitively, the fourth trajectory is selected, which is the coupling displacement data under the condition that the motions in three directions produce input. For better comparative analysis, the coupling displacement on the y-axis is taken as a negative sign. The results are shown in Fig.12.

Through Fig.12, it can be found that the coupling displacement generated in the x-axis is slightly larger than that generated in the y-axis under the given fourth level sea condition, and the maximum X_c is 286.4214mm, the maximum Y_c is 275.8547mm, and the maximum Z_c is 128.7035mm. The coupling displacement in the z-axis can be offset by the control strategy.

V. CONCLUSION

In this article, constructed a 3-DOF parallel platform based on the 3UPU parallel platform with 5-DOF, by adding a UP followed limb. The platform is a kind of coupled 3-DOF platform, which will produce coupling displacement in the direction of the x-axis, y-axis, and z-axis. The DOFs and the mobility of the platform are analyzed by the screw theory. The coupling constraint equation of the platform is obtained by the coordinate transformation method. The inverse and forward solutions of the displacement kinematics of the platform are analyzed, and the motion trajectory of the platform is obtained, which verifies the correctness of the constraint equation. The coupling displacement is related to the structure size and input parameters of the platform. By using the characteristics of coupling displacement, more freedom of motion can be compensated. It can be used as a stable platform for helicopter landing and cargo transfer.

In future research, experiments will be added to measure the actual coupling displacement of the platform in the process of moving.

REFERENCES

[1] K. M. Lynch and F. C. Park, *Modern Robotics: Mechanics, Planning, and Control*. Cambridge, U.K.: Cambridge Univ. Press, 2017.

[2] L. Wang, H. Xu, and L. Guan, "Optimal design of a 3-PUU parallel mechanism with 2R1T DOFs," *Mechanism Mach. Theory*, vol. 114, pp. 190–203, Aug. 2017.

[3] S. Lu, B. Ding, and Y. Li, "Minimum-jerk trajectory planning pertaining to a translational 3-degree-of-freedom parallel manipulator through piecewise quintic polynomials interpolation," *Adv. Mech. Eng.*, vol. 12, no. 3, pp. 1–18, 2020.

[4] S. Lu, Y.-M. Li, and B.-X. Ding, "Multi-objective dimensional optimization of a 3-DOF translational PKM considering transmission properties," *Int. J. Autom. Comput.*, vol. 16, no. 6, pp. 748–760, Dec. 2019.

[5] T. Liu, Y. Hu, H. Xu, Q. Wang, and W. Du, "A novel vectored thruster based on 3-RPS parallel manipulator for autonomous underwater vehicles," *Mechanism Mach. Theory*, vol. 133, pp. 646–672, Mar. 2019.

[6] T. Zheng, F. Zheng, X. Rui, L. Yan, K. Niu, and F. Zhang, "Analysis of a three-extensible-rod tracker based on 3-RPS parallel manipulator for space large deployable paraboloid structure with power and communication integration," *Acta Astron.*, vol. 169, pp. 1–22, Apr. 2020.

[7] Z. Huang and Q. Li, "Construction and kinematic properties of 3-UPU parallel mechanisms," in *Proc. Int. Design Eng. Tech. Conf. Comput. Inf. Eng. Conf.*, vol. 36533, 2002, pp. 1027–1033.

[8] Z. Huang, J. Liu, and D. Zeng, "A general methodology for mobility analysis of mechanisms based on constraint screw theory," *Sci. China E, Technol. Sci.*, vol. 52, no. 5, pp. 1337–1347, May 2009.

[9] R. Di Gregorio and V. Parenti-Castelli, "Mobility analysis of the 3-UPU parallel mechanism assembled for a pure translational motion," *J. Mech. Design*, vol. 124, no. 2, pp. 259–264, Jun. 2002.

[10] D. Zhang and B. Wei, "Interactions and optimizations analysis between stiffness and workspace of 3-UPU robotic mechanism," *Meas. Sci. Rev.*, vol. 17, no. 2, pp. 83–92, Apr. 2017.

[11] B. Aboulissane, D. E. Haiek, and L. E. Bakkali, "3-UPU robotic mechanism performance evaluation through kinematic indexes," *Procedia Manuf.*, vol. 22, pp. 468–475, Jan. 2018.

[12] S. Yang and Y. Li, "Different kinds of 3T2R serial kinematic chains and their applications in synthesis of parallel mechanisms," *Mechanism Mach. Theory*, vol. 144, pp. 1–12, Feb. 2020.

[13] S. Sarabandi, P. Grosch, J. M. Porta, and F. Thomas, "A reconfigurable asymmetric 3-UPU parallel robot," in *Proc. Int. Conf. Reconfigurable Mech. Robots (ReMAR)*, Jun. 2018, pp. 1–8.
[14] Z. Huang and Q. C. Li, "Type synthesis of symmetrical lower-mobility parallel mechanisms using the constraint-synthesis method," *Int. J. Robot. Res.*, vol. 22, no. 1, pp. 59–79, Jan. 2003.
[15] S. El Hraiech, A. H. Chebbi, Z. Affi, and L. Romdhane, "Genetic algorithm coupled with the Krawczyk method for multi-objective design parameters optimization of the 3-UPU manipulator," *Robotica*, vol. 38, no. 6, pp. 1138–1154, Jun. 2020.
[16] Y. Li and Q. Xu, "Kinematic analysis of a 3-PRS parallel manipulator," *Robot. Comput.-Integr. Manuf.*, vol. 23, no. 4, pp. 395–408, Aug. 2007.
[17] G. Bhutani and T. A. Dwarakanath, "Practical feasibility of a high-precision 3-UPU parallel mechanism," *Robotica*, vol. 32, no. 3, pp. 341–355, May 2014.
[18] Y. Lu, Y. Shi, and B. Hu, "Kinematic analysis of two novel 3UPU I and 3UPU II PKMs," *Robot. Auto. Syst.*, vol. 56, no. 4, pp. 296–305, Apr. 2008.
[19] M. Shafiee-Ashtiani, A. Yousefi-Koma, S. Iravanimanesh, and A. S. Bashardoust, "Kinematic analysis of a 3-UPU parallel robot using the ostrowski-homotopy continuation," in *Proc. 24th Iranian Conf. Electr. Eng. (ICEE)*, May 2016, pp. 1306–1311.
[20] C. Yang, Z. Qu, and J. Han, "Decoupled-space control and experimental evaluation of spatial electrohydraulic robotic manipulators using singular value decomposition algorithms," *IEEE Trans. Ind. Electron.*, vol. 61, no. 7, pp. 3427–3438, Jul. 2014.
[21] J. A. Carretero, R. P. Podhorodeski, M. A. Nahon, and C. M. Gosselin, "Kinematic analysis and optimization of a new three degree-of-freedom spatial parallel manipulator," *J. Mech. Design*, vol. 122, no. 1, pp. 17–24, Mar. 2000.
[22] E. Luo, D. Mu, X. Liu, and T. Zhao, "A 3-DOF coupling parallel mechanism for stabilized platform and its motion characteristics," *Robot*, vol. 32, no. 5, pp. 681–687, 2010.
[23] S. Chandrasekaran and R. Nagavinothini, "Tether analyses of offshore triceratops under wind, wave and current," *Mar. Syst. Ocean Technol.*, vol. 13, no. 1, pp. 34–42, Mar. 2018.
[24] Q. Zhang, H. Zhai, P. Wang, S. Wang, L. Duan, L. Chen, Y. Liu, and D.-S. Jeng, "Experimental study on irregular wave-induced pore-water pressures in a porous seabed around a mono-pile," *Appl. Ocean Res.*, vol. 95, pp. 1–14, Feb. 2020.

XIONG HU received the bachelor's and Ph.D. degrees from Shanghai Jiao Tong University. He was a Visiting Professor with the Queensland University of Technology, Australia. He serves as the Executive Director of the Shanghai Mechanical Engineering Society, the Chairman of the Committee of Equipment Condition Monitoring, Assessment and Strategic Decision of the Shanghai Mechanical Engineering Society, and the Deputy Director of limb of the Health Condition Monitoring of Shanghai Equipment Management Association. He is currently a Professor and a Ph.D. Supervisor with Shanghai Maritime University (SMU), the Dean of the Logistics Engineering College, SMU, and the Dean of the Sino-Dutch Mechatronics Engineering College, SMU. He was responsible for or participated in almost 100 research projects which were sponsored by National Funding Programs, government and both here and abroad enterprises, such as NNSF, 863 Program, Dubai Aluminium Company Ltd., Port of Damman, Port of Shanghai, Shanghai Bao Steel Company, ZPMC, and BV. His current research interests include, research and teaching works, (health) condition monitoring, (remote) control, (condition) assessment, and (maintenance) management of large equipment and its structure, and intelligent processing and prediction of health condition data and signals of machines. In recent years, his major research interests include technique development and its application of health condition management, fault diagnosis, safety assessment, and integrated online system of the large hoisting appliances, such as cranes and logistics equipments.

FURONG LI is currently pursuing the master's degree in mechanical engineering with Shanghai Maritime University, Shanghai, China. He has applied for five utility model patents and two invention patents. His research interests include six-DOF wave compensation platform and motion prediction of wave compensation platform.

GANG TANG received the master's degree in mechanical engineering from the Harbin Institute of Technology and the Ph.D. degree in mechanical engineering from Shanghai Jiao Tong University. He joined the Faculty at Shanghai Maritime University, where he is currently an Associate Professor with the Department of Mechanical Engineering. He has been in charge of more than ten Programs and participated in more than 15 Programs. He has published 36 articles and holds nine patents awarded. His research interest includes ocean engineering.